Feedback between rifting and diapirism can exhume ultrahigh-pressure rocks

Article *in* Earth and Planetary Science Letters · November 2011

DOI: 10.1016/j.epsl.2011.09.031

5 authors, including:

Susan Ellis
GNS Science
95 PUBLICATIONS **1,803** CITATIONS
SEE PROFILE

Bradley Hacker
University of California, Santa Barbara
303 PUBLICATIONS **11,773** CITATIONS
SEE PROFILE

Earth and Planetary Science Letters 311 (2011) 427–438

Contents lists available at SciVerse ScienceDirect

Earth and Planetary Science Letters

journal homepage: www.elsevier.com/locate/epsl

Feedback between rifting and diapirism can exhume ultrahigh-pressure rocks

S.M. Ellis [a,*], T.A. Little [b], L.M. Wallace [a], B.R. Hacker [c], S.J.H. Buiter [d]

[a] GNS Science, P.O. Box 30368, Lower Hutt 5010, New Zealand
[b] School of Geography, Environment and Earth Sciences, Victoria University of Wellington, Wellington 6040, New Zealand
[c] Earth Science, University of California, Santa Barbara, CA 93106-9630, USA
[d] Geological Survey of Norway, Leiv Eirikssons vei 39, 7491 Trondheim, Norway

ARTICLE INFO

Article history:
Received 11 April 2011
Received in revised form 19 September 2011
Accepted 20 September 2011
Available online 6 November 2011

Editor T.M. Harrison

Keywords:
ultrahigh-pressure
rock exhumation
diapir
rift
extension
Woodlark Basin

ABSTRACT

The processes by which crustal rocks are buried to tremendous depths and subsequently exhumed to Earth's surface remain controversial. Rapid exhumation of Earth's youngest (ultra-) high-pressure (UHP) rocks in the Woodlark Basin, Papua New Guinea, is occurring within an active rift, in contrast to more common scenarios of UHP exhumation during plate convergence. We use 2D and 3D thermo-mechanical models to demonstrate that UHP exhumation can result from feedback between rifting and the diapiric rise of a previously subducted continental fragment through the lithosphere. We infer that this feedback is responsible for the exhumation of the UHP rocks in gneiss domes in the Woodlark Basin. Our models successfully reproduce UHP exhumation paths and rates, and geological structures within the gneiss domes. We show that UHP exhumation by diapirism is mechanically consistent in post-collisional rifts. Our models highlight the complex feedback between diapiric ascent and extension.

1. Introduction

One of the most exciting questions in the study of continental dynamics is how some crustal rocks are buried to tremendous depths (>100 km) to be subsequently exhumed to Earth's surface. Recent widespread discoveries of "ultrahigh-pressure" (UHP) terranes, characterised by the presence of coesite and, in some cases, diamond (Chopin, 1984; Dobrzhinetskaya et al., 1995), assemblages which form at pressures of 3–5 GPa (equivalent to depths of 90–150 km), have led to proposals that large bodies of buoyant continental crust have repeatedly been subducted to mantle depths. The large volume of ancient UHP and high pressure (HP; forming under lithostatic pressures equivalent to 60–90 km depth) terranes identified worldwide implies that subduction and exhumation of continental crust has had a major impact on Earth evolution. Although many studies agree that UHP rocks may be created by the subduction of continental crust (e.g., Andersen and Jamtveit, 1990; Chopin, 2003; Gerya and Stockhert, 2006; Liou et al., 2004; Smith, 1984; Warren et al., 2008) the processes leading to the *exhumation* of UHP terranes remain uncertain or variable (e.g., Burov et al., 2001; Gerya and Stockhert, 2006; Hacker, 2007; Li and Gerya, 2009; Vrijmoed et al., 2009; Warren et al., 2008). Many of these terranes have been raised from mantle depths at plate–tectonic rates of centimetres per year (Amato et al., 1999; Baldwin et al., 2004; Hermann et al., 2001; Parrish et al., 2006).

The world's youngest UHP terrane is in the D'Entrecasteaux Islands of the Woodlark Basin, Papua New Guinea. There, HP and coesite-bearing UHP eclogites have been exhumed at cm/yr rates in only the past few million years — a process that is thought to be continuing today in an active rift setting (Baldwin et al., 2004, 2008; Little et al., 2011) (Fig. 1; Supplementary Fig. S1). The HP and UHP rocks are part of a coherent metamorphic terrane, mostly felsic in composition, that is exposed in several gneiss domes (20–30 km in diameter) preserving abundant evidence of synexhumational partial melting (Davies and Warren, 1988; Hill et al., 1995; Little et al., 2011). The burial of these continental-affinity (Australian Plate-derived (Baldwin and Ireland, 1995)) rocks to mantle depths is thought to have occurred by attempted subduction of the leading edge of a continental fragment at the NE margin of the Australian Plate beneath the Papua New Guinea mainland during an arc–continent collision that began ~58 Ma (Lus et al., 2004). Intriguingly however, the currently preserved (radiometrically dated) eclogite-facies crystallisation of the UHP terranes, and their subsequent rapid exhumation did not take place until the late Miocene to Pliocene (~8–4 Ma, Baldwin et al., 2004; Monteleone et

* Corresponding author.
E-mail addresses: s.ellis@gns.cri.nz (S.M. Ellis), tim.little@vuw.ac.nz (T.A. Little), l.wallace@gns.cri.nz (L.M. Wallace), hacker@geol.ucsb.edu (B.R. Hacker), susanne.buiter@ngu.no (S.J.H. Buiter).

al., 2007), long after the collision, but simultaneous with westward propagation of the Woodlark Rift (a still-active zone of active continental extension and seafloor spreading) into the upper plate of the defunct Papuan collisional orogen (Benes et al., 1994; Goodliffe et al., 1997; Taylor et al., 1999). Given that the D'Entrecasteaux Islands UHP terrane occurs within a well-documented extensional rift setting, the exposure of the world's *only* actively exhuming UHP rocks cannot be explained by the most commonly invoked class of UHP exhumation models: syn-convergent extrusion or return flow of the HP and UHP rocks to the surface in a still-active subduction channel (e.g., Burov et al., 2001; Gerya and Stockhert, 2006; Hacker et al., 1995; Li and Gerya, 2009; Warren et al., 2008).

Using numerical models, we test whether exhumation of the (ultra-) high-pressure D'Entrecasteaux rocks might have occurred by the rise of felsic diapirs (Little et al., 2011); and, if so, under what conditions. Using modern-day plate tectonic boundary conditions, we demonstrate that rapid vertical ascent of partially molten felsic crustal bodies within a rift setting is a mechanically feasible process that can account for the observed exhumation history and field structures of the rocks. Most importantly, we show that rifting of

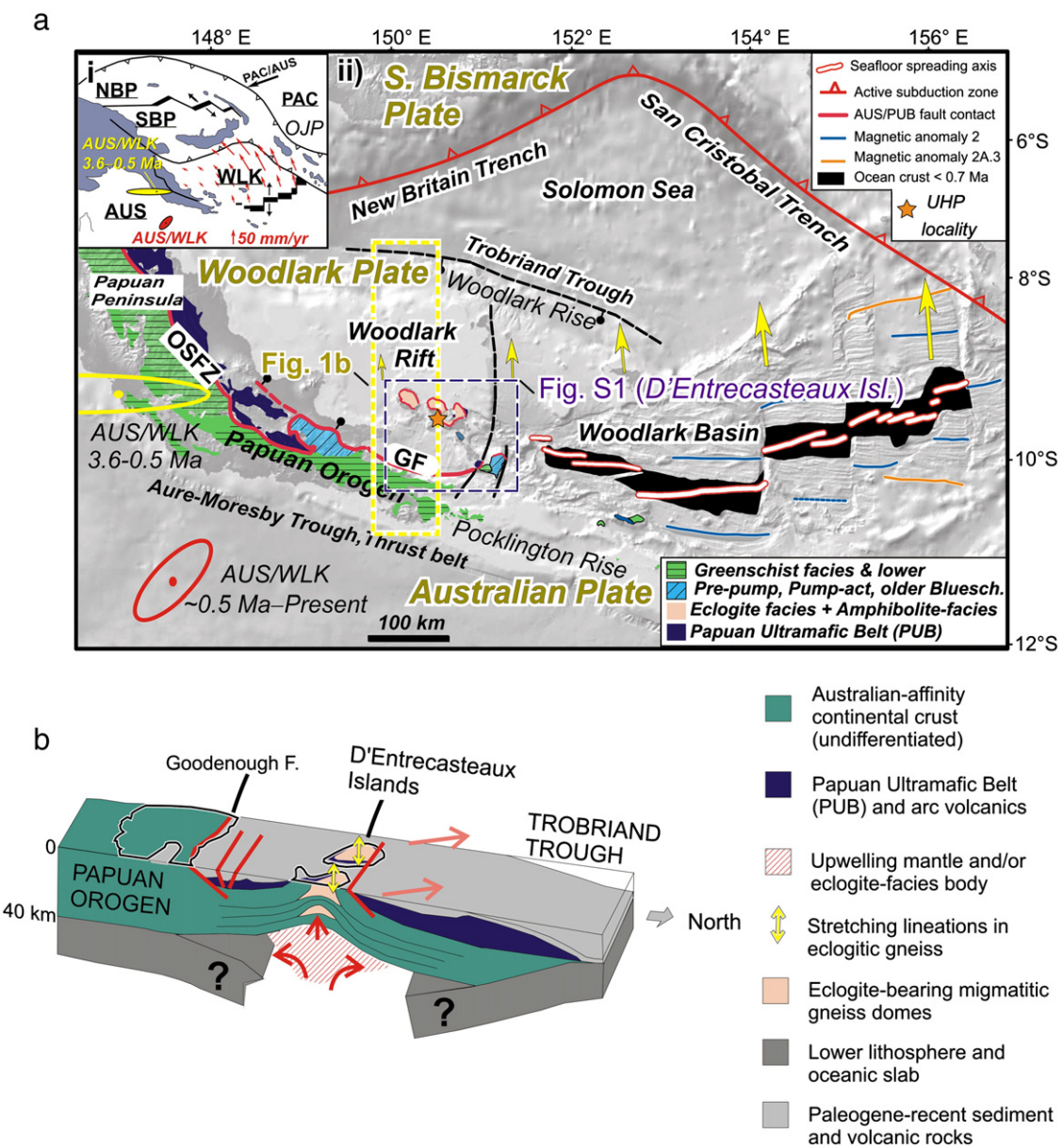

Fig. 1. Tectonic setting of the D'Entrecasteaux Islands and Woodlark Rift, Papua New Guinea. (a) Inset (i): contemporary plate tectonic map of eastern Papua New Guinea: NBP, North Bismarck Plate, SBP, South Bismarck Plate, WLK, Woodlark Plate, AUS, Australian Plate, PAC, Pacific Plate; OJP, Ontong-Java Plateau. Bold black arrow shows velocity of the Pacific Plate relative to the Australian Plate. Small red arrows depict velocities of the Woodlark Plate relative to the Australian Plate after Wallace et al. (2004). All velocity magnitudes are shown relative to 50 mm/yr key at bottom right of inset. (ii) Simplified tectonic map of southeastern Papua New Guinea modified after Webb et al. (2008), showing key tectonic features and distribution of metamorphic rocks. Background is shaded Digital Elevation Model from GeoMapApp (http://www.GeoMapApp.org). Geologic units are much simplified from Daczko et al. (2009) and Davies (1980b). Pre–pump = prehnite–pumpellyite facies; Pump–act = pumpellyite–actinolite facies. Pole of WLK–AUS rotation for 3.6–0.5 Ma (with error ellipse) from Taylor et al., 1999; GPS-derived pole of present-day WLK–AUS rotation from Wallace et al. (2004). Explanation: OSFZ, Owen Stanley fault zone; GF, Goodenough normal fault. Magnetic anomalies from Taylor et al. (1999). Yellow vectors indicate eastward increase in velocity associated with 3.6–0.5 Ma pole of rotation, used in this study. Yellow and blue dashed boxes outline areas shown in Fig. 1b and Supplementary Fig. S1, respectively. (b) Schematic block-model for present-day setting of D'Entrecasteaux Islands and Woodlark Basin tectonics, modified after Hill et al. (1995), Little et al. (2011), and Webb et al. (2008). Bold red lines: main active faults. Yellow double arrows: ductile stretching lineation directions in gneiss domes. Pink arrows: extension directions 3.6–0.5 Ma.

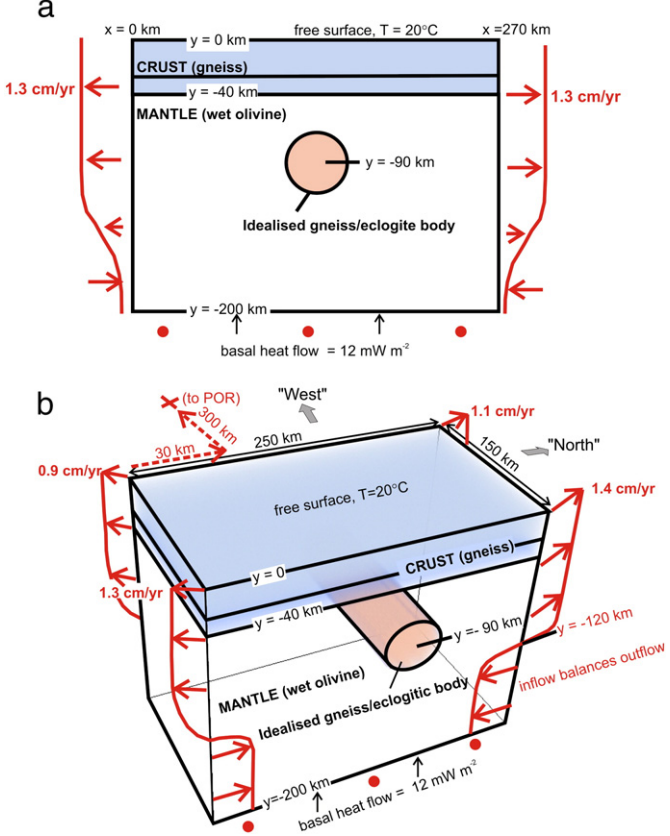

Fig. 2. Setup for the numerical models. (a) 2D model initial and boundary conditions. No vertical exaggeration. (b) 3D model initial and boundary conditions. Inflow velocity boundary conditions are prescribed to give zero net influx into model box. "to POR" means 300 km to the pole of rotation. For details of material properties, see Table 1 and Supplementary Note S1.

the overlying lithosphere and diapiric rise of quartzofeldspathic terranes positively reinforce each other to promote exhumation at plate–tectonic rates.

2. Tectonic setting and summary of relevant constraints on timing and style of exhumation in the Woodlark Basin

The Woodlark Basin is part of a complex convergent plate boundary zone between Australian and Pacific lithosphere involving small microplates and continental fragments (Fig. 1a). In the Papuan Peninsula, an arc–continent collision caused southwestward obduction of a Cretaceous ophiolite, the Papuan Ultramafic Belt (PUB) over sediments and volcanic rocks accreted from the downgoing Australian margin that began by 58 Ma, the age of the high-temperature metamorphic sole at the base of the ophiolite (Davies and Jacques, 1984; Lus et al., 2004; Van Ufford and Cloos, 2005). An apparent cessation of this collision by 35–30 Ma is recorded by the subsequent shedding of thick clastic wedges derived from the erosional unroofing of the PUB and the underlying Owen Stanley metamorphic rocks; these were transported southward into the Moresby Trough (the trench of the now extinct Papuan subduction zone) and northward into the Trobriand Basin, followed by Miocene orogenic subsidence (Davies, 1990; Davies and Jacques, 1984; Rogerson et al., 1987; Taylor and Huchon, 2002; Van Ufford and Cloos, 2005). The gently NE-dipping dense PUB layer, up to 20-km thick, was emplaced southwestward along the Owen Stanley Fault zone (OSFZ). After this collision, southward subduction of Solomon Sea lithosphere at the Trobriand Trough may have begun north of the body. An active oceanic spreading centre in the Woodlark Basin began propagating westward between the continental Pocklington and Woodlark Rises at 6–8 Ma (Taylor et al., 1999), and, to the northeast, links up to the New Britain and San Cristobal trenches, which now take up a large component of the convergent motion between the Australian and Pacific plates (Tregoning et al., 1998; Wallace et al., 2004). From seafloor spreading data, the Woodlark Plate is inferred to rotate anticlockwise at ~4.23°/Myr about a nearby pole of rotation located at 9.4°S, 147°E from 3.6 to 0.5 Ma (Taylor et al., 1999), while geodetic studies suggest the current pole of rotation for the Woodlark plate is located at 11.3°S, 147.6°E, with an anticlockwise rotation rate of 2.8°/Myr (Wallace et al., 2004). Geodetically-derived modern-day rates of rifting are ~1–2 cm/yr in the western Woodlark Basin where the UHP rocks are currently being exhumed, while the rates of rifting increase to ~4 cm/yr in the eastern Woodlark Basin at ~155°E due to rotation of the Woodlark Plate about a nearby pole.

On the mainland, during the late Cenozoic, the PUB has been cut by the active Goodenough Fault along the southern margin of Goodenough Bay (Mutter et al., 1996; Spencer, 2010). The latter is a rapidly slipping, active normal fault that bounds the Dayman Dome on its footwall, and it is a major element of the current Australian–Woodlark plate boundary zone (Daczko et al., 2009; Spencer, 2010).

The gneiss domes of the D'Entrecasteaux Islands expose a coherent terrane of amphibolite-facies gneiss containing retrogressed HP/UHP eclogite ("lower plate"); the domes have an upper mylonitic carapace and have been emplaced against an overlying body ("upper plate") of ophiolitic serpentinised ultramafic rocks and gabbro of the Papuan

Table 1
Thermal and mechanical properties of 2D and 3D models.

Gravitational acceleration ($m\,s^{-2}$)	9.81
Thermal conductivity ($Wm^{-1}\,K^{-1}$)	2.48
Heat capacity ($kJ\,kg^{-1}\,K^{-1}$)	1
Volumetric heat production (Wm^{-3})	0 (mantle), 10^{-7} (lower crust), 7.67×10^{-7} (upper crust and imposed body)
Basal heat-flow ($mW\,m^{-2}$); surface temperature (°C)	12; 0
Lower and upper bounds on effective viscosity (Pa s)	5×10^{18}; 5×10^{23}
Angle of internal friction (softened between 20 and 50% brittle strain)	25° (softening linearly to 5) crust([1]); 25° (no softening) mantle
Cohesion (MPa) (softened between 20 and 50% brittle strain)	15 (softening linearly to 3) crust; 1 mantle
Crustal power–law creep parameters: pre-exponential constant ($Pa^{-n}s^{-1}$), power–law exponent n, activation energy ($kJ\,mol^{-1}$)	5×10^{-24}; 3; 190 ([2])
Mantle power–law creep parameters: pre-exponential constant ($Pa^{-n}s^{-1}$), power–law exponent n, activation energy ($kJ\,mol^{-1}$)	7×10^{-14}; 3; 520 ([3])
Reference mantle density ($kg\,m^{-3}$) and thermal expansion coefficient (K^{-1}); compressibility coefficient (Pa^{-1})	3370; 2.65×10^{-5}; 10^{-11} ([4])

[1] The unsoftened and softened values of internal friction are lower than Byerlee's law, since effects of hydrostatic fluid pressure are implicitly included in friction angle.
[2] Quartz; Brace and Kohlstedt (1980) (chosen for compatibility with models of Rey et al., 2009).
[3] Dry olivine; Goetze (1978) (chosen for compatibility with models of Rey et al., 2009).
[4] Dziewonski and Anderson (1981).

Ultramafic Belt (Davies and Warren, 1988). The ophiolite has been subject to at most low-grade metamorphism and is overlain by a sequence of unmetamorphosed sedimentary and volcanic rocks of late Miocene and younger age. Some of these strata were being deposited when the "lower plate" rocks resided at mantle depths, and yet now the two units (upper and lower plates) are tectonically juxtaposed. The ca. 20 km-diameter domes reach elevations of over 2000–2500 m, are flanked on their northern (and locally southern) sides by active normal faults, and are inferred to be part of a coherent UHP terrane that is continuous at depth (Little et al., 2007, 2011) (Fig. 1; Supplementary Fig. S1). Peak (U)HP metamorphism, with temperatures of up to ~900 °C and pressures as high as 2.7 GPa (Baldwin et al., 2004, 2008; Monteleone et al., 2007), occurred at 8–4 Ma (east and central regions) to as young as ~2 Ma (west), suggesting exhumation rates of >2–3 cm/yr from depths of 40–90 km (ion-probe U–Pb geochronology by Baldwin et al., 2004, 2007). The exhumation-related lower crustal deformational fabrics, the abundance of partially molten rock, and the pattern of cooling ages, indicate that the most deeply exhumed rocks occur roughly in the centres of the migmatitic gneiss domes grades rather than adjacent to the (late-stage) normal faults bounding their margins (Little et al., 2011). Stretching lineations interpreted to represent late-stage ductile deformation in the domes have a complex 3D pattern, with dominant east–west trends near the centre of the domes rotating to south-trending farther away from the dome centres near the south-west coasts (Fig. 1b; Supplementary Fig. S1). The east–west ductile stretching directions in the domes, approximately parallel to the rift margins, are contrary to the expected orientation (parallel to the extension direction) if ductile deformation mirrored that seen at the surface.

Geological and thermochronological reconstructions indicate a progression in extension and exhumation from east to west, similar to the westward propagation direction of the Woodlark seafloor spreading and continental crust rifting. Such trends include a westward younging of late Miocene to Pliocene UHP metamorphic ages and also of low-temperature thermochronometric cooling ages (Fitzgerald et al., 2008).

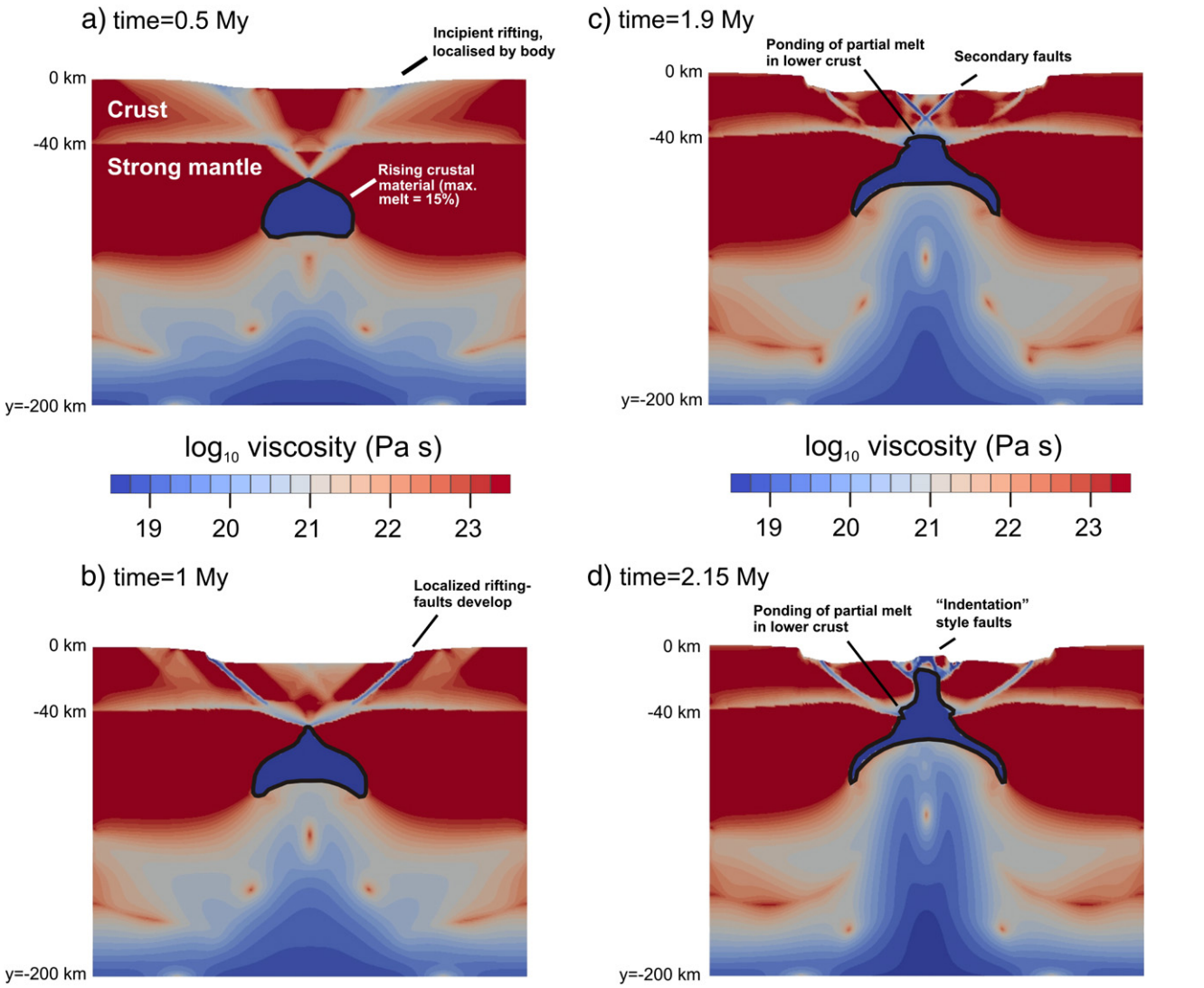

Fig. 3. Results of a simple, symmetric 2D numerical model. The model setup is shown in Fig. 2a. Black bold lines outline eclogite-facies continental-affinity body emplaced at depth. No vertical exaggeration. (a–e) Time sequence showing colour contours of log10 (effective viscosity). Warm colours indicate more viscous regions in upper crust and mantle, as determined naturally by the model according to ambient temperatures and strain rates. (f) (i) Colour contours of brittle strain after 2.3 My of extension. (ii) Colour contours of melt fraction after 2.3 My of extension. Note that the model has unnatural topography (e.g., slopes of >45°). This results from the limited grid resolution, relatively high surface cohesion necessary for numerical convergence near the surface, and lack of sedimentation and erosion. We have also neglected small-scale strength perturbations in the crust and mantle which will tend to distribute extension over a greater area. The slight asymmetry in faulting pattern that develops in the model is caused by small numerical discretisation errors in accumulated strain (model initial and boundary conditions are symmetric).

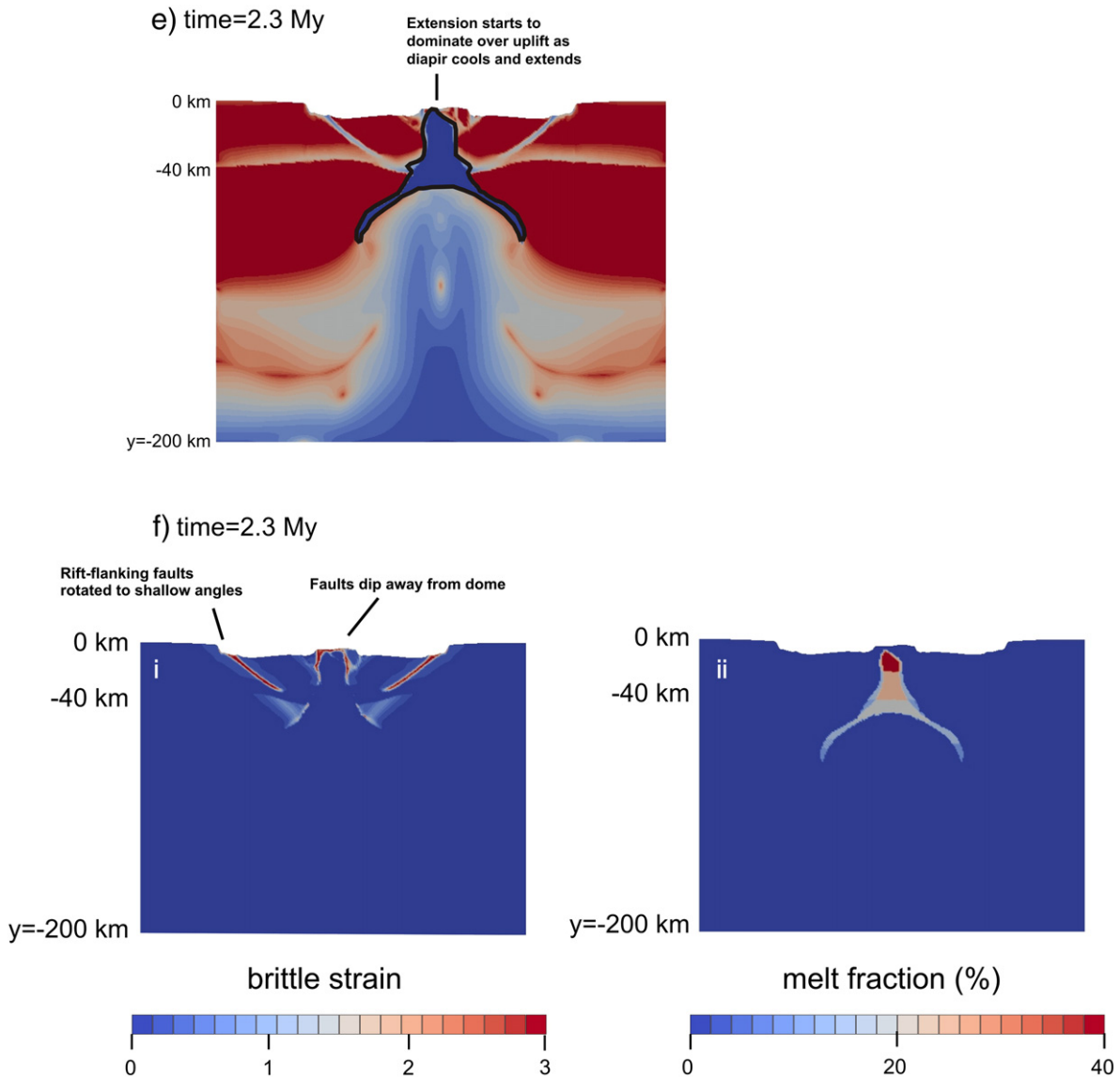

Fig. 3 (*continued*).

3. Modelling approach for 2D and 3D finite-element models

3.1. Model setup and rheology

The numerical modelling is performed using the thermo-mechanical code SULEC (developed by Susan Ellis and Susanne Buiter) which solves the incompressible Stokes equation for slow creeping flow together with the heat equation. Thermal diffusion and advection are computed at each timestep. Pressure (mean stress) is calculated through an iterative penalty formulation (Pelletier et al., 1989). The Eulerian grid on which the computation is performed does not deform horizontally but stretches vertically to account for topographic changes at the upper free surface. Materials, strain and stress fields are advected via tracer particles. In the first model described in this paper, the modelled domain in 2D is 270 km wide and 200 km deep with a grid resolution of 1 km (a total of 54,000 elements) and ca. 4 tracer particles per element (Fig. 2a). In 3D the model is 250×200×150 km with an average crustal grid resolution of 3 km, a coarser grid resolution in the mantle (a total of 130,000 elements), and an average of 8 tracer particles per element. The elements are quadrilaterals with 2 degrees of freedom (d.o.f.) for corner node velocity in 2D (3 d.o.f. per node in 3D) with constant pressure (Fig. 2b).

Thermal and material parameters are detailed in Table 1. The model rheology accumulates brittle strain according to a Coulomb yield criterion, a process that gives way to thermally-activated dislocation creep at higher temperatures, depending on crustal and mantle compositions. That is, we apply a rheology that is a combination of power–law viscous creep and frictional plasticity, where the brittle–ductile transition is determined at each step according to the lowest predicted differential stress for the two mechanisms (e.g., Fullsack, 1995). We assume that crustal rocks weaken with strain to represent effects of brittle fault development and softening due to, for example, cohesion loss, mineral phase changes, elevated pore fluid pressures, grain size reduction and/or the development of foliation. The models do not include frictional strain softening in the mantle, but we discuss the sensitivity of this assumption in Section 4.1.

Viscosities in the crust and deep body are modified where melt is present according to Supplementary Note S1, which is based on the relative fall-off in viscous strength after Rosenberg et al. (2007). A

lookup table based on pseudosection calculations from Perple_X (Connolly and Petrini, 2002) is used to compute the evolution in melt fraction and density for the exhuming crustal body and overlying continental crust assuming 5% volume D'Entrecasteaux Islands mafic eclogite and 95% volume quartzofeldspathic gneiss with 2 wt.% H_2O (Supplementary Note S1). When melt is present at the calculated pressure and temperature, latent heat is included in the thermal calculation via an increased effective heat capacity (Gerya and Yuen, 2003; Supplementary Note S1).

The upper crust and lower crust are initially 25 and 15 km thick. The model starts with a 22-km-radius subducted body of continental affinity, centred at a depth of 90 km (minimum depth of coesite stability), that had become detached from denser, subducted lithosphere with which it had been subducted into the mantle during the previous Papuan arc–continent collision. A circular shape is assumed for the subducted body, though supplementary models investigate the effects of other less symmetric shapes. In 3D, this body extends along the z-axis as a right circular cylinder at a uniform depth of 90 km. The frictional and creep strength of the subducted body are assumed to be the same as the crust.

The initial thermal field is determined by solving the steady-state heat equation assuming no heat-flow at the side boundaries and the thermal properties of Table 1. Solving for these parameters gives a cool initial thermal gradient averaging 6 °C km^{-1} (9.5 to 10.5 °C km^{-1} in the crust, where the slightly higher gradient is directly above the body owing to more heat production there). The imposed body starts with temperatures between 700 and 900 °C, consistent with the temperatures recorded during peak metamorphism in (U)HP rocks now at the surface (Baldwin et al., 2004, 2008). Moho temperature ranges from 380 °C to 420 °C directly above the body. The low average initial geotherm is consistent with cooling due to the prior subduction phase for the Woodlark Basin. We assume (after Little et al., 2011) that any syn-collisional (Paleogene) UHP assemblages that may originally have been present were later recrystallised in the late Neogene. Post-collisional conditions that might have delayed final UHP crystallisation until the late Neogene – and prevented melting of the subducted continental material during the intervening ~20–25 Myr – might have included a) the body being large enough to avoid significant conductive heating (i.e., >25 km in width), or b) cool conditions continuing to prevail in the

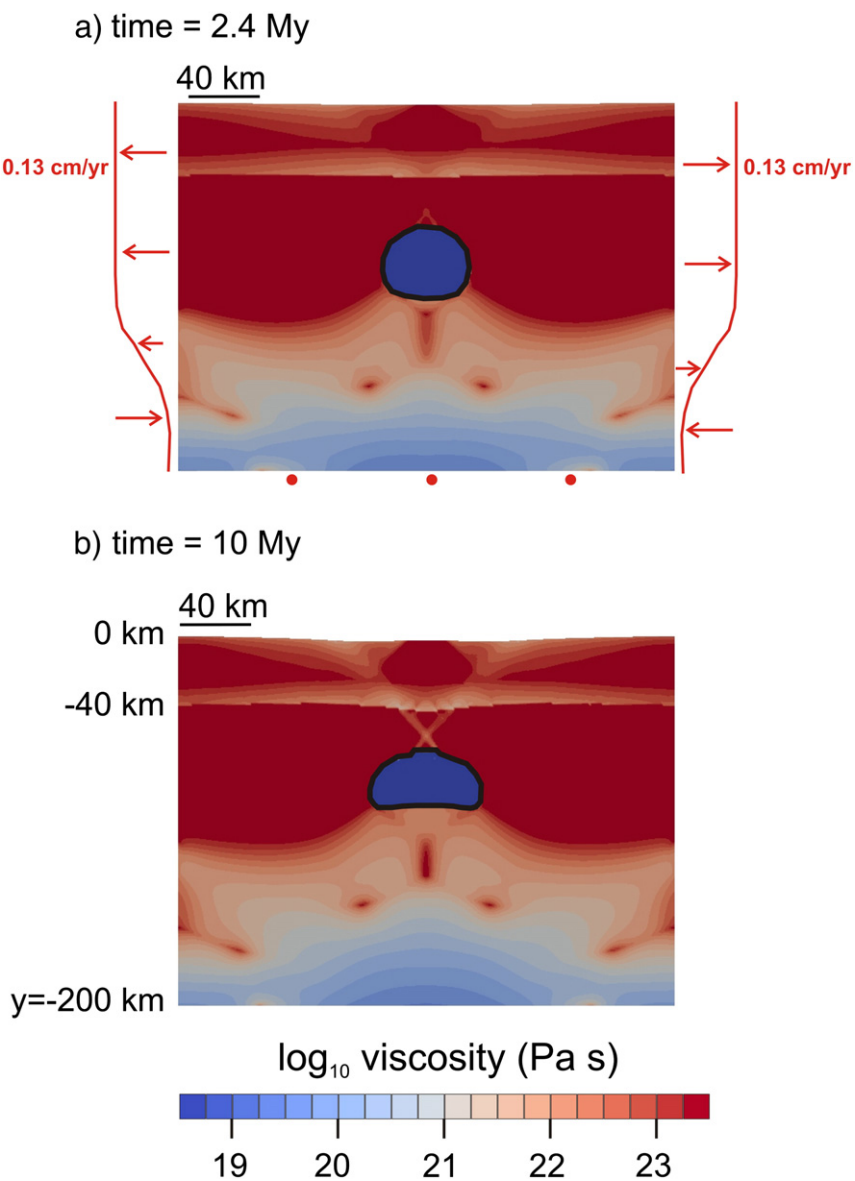

Fig. 4. Results for a 2D numerical model with the same setup as that shown in Fig. 2a, but a much lower extension rate. Symmetric extension in the top 120 km is 0.26 cm yr^{-1} i.e. 10× slower than results in Fig. 3. (a–b) time sequence log10 (effective viscosity), illustrating that with little extension, diapiric rise of a partially molten body is impeded.

paleosubduction zone, perhaps arising from southward subduction of Solomon Sea lithosphere along the Trobriand Trough (Fig. 1) to the north in the Miocene (e.g., Taylor and Huchon, 2002; Van Ufford and Cloos, 2005) by subduction refrigeration (Hacker and Peacock, 1994). Alternatively, c) some reactivated shortening and subduction along the old suture in the late Miocene–early Pliocene (e.g., van Ufford and Cloos, 2005) might have transported Paleogene subducted materials to greater depth, causing them to recrystallise for the first time at (U)HP conditions. Which, if any, of these "pressurisation" models is correct is beyond the scope of this paper. The conceptual model preferred by Little et al. (2011) infers that reheating and fluid influx related to the Woodlark rifting caused the final stage of Late Neogene (U)HP metamorphic recrystallisation in the older subducted continental materials, which overprinted original Paleogene-aged metamorphic assemblages that are now only locally preserved (Zirakparvar et al., 2009, 2010, and manuscript in review). What is important here is that it is well established (Baldwin et al., 2004; Monteleone et al., 2007) that the rocks were crystallised in the eclogite-facies in the late Neogene, and that this paper is concerned with the process of their subsequent exhumation.

The low geothermal gradient of the initial models is similar to that which may have existed during the Paleogene Papuan arc–continent collision that originally carried the body northwards to depth, and which resulted in blueschist-facies crystallisation in the Owen-Stanley metamorphic rocks on the mainland (Daczko et al., 2009; Davies and Jacques, 1984). Our starting temperatures and pressures for the UHP body agree with published thermobarometric determinations for those rocks based on coexisting minerals in the eclogites prior to their rapid exhumation (Baldwin et al., 2004, 2008; Monteleone et al., 2007).

No surface erosion or sedimentation is applied. 2D boundary conditions impose a symmetric total extension rate of 2.6 cm yr^{-1} along the upper 120 km model sides (Taylor et al., 1999; Wallace et al., 2004) (Fig. 2a), which is mass-balanced by inflow boundary conditions between depths of 120–200 km; experiments have shown that side inflow has a less pronounced effect on the surface deflection in the models, and is consistent with earlier rifting models (e.g., Buiter et al., 2009). The base has free horizontal slip and the top is a free surface with isostatic stabilisation (Kaus et al., 2010; Quinquis et al., 2011). In 3D, the boundary conditions are similar (with inflow balancing outflow) but the imposed velocity is applied according to a pole of rotation located 300 km behind the model and 30 km north of its southern edge (Fig. 2b). This gives total extensional velocities of 2.7 and 2 cm yr^{-1} along the front and back of the model, respectively. Along the front and back surfaces, the boundary velocity direction is constrained to be consistent with the pole of rotation though otherwise freely determined.

4. Results

4.1. 2D model results

Fig. 3 shows the results of a simple two-dimensional model, which investigates the interplay between rift extension and the diapiric rise of a buried UHP continental crustal body. We use a setup simplified from conditions inferred to exist after the end of continental subduction in the early Miocene as described in Sections 2 and 3.

During the first ca. 0.5 Myr after the onset of extension (start of the model), the low density of the deep-seated, partially-molten, felsic body causes it to rise buoyantly to the base of the strong lithospheric upper mantle, a distance of ca. 15 km at a mean ascent rate of 2.7 cm/yr (Fig. 3a). Extension in the strong, overlying frictional upper mantle and crust of the rift begins to localise above the partially molten UHP body. This localisation is caused by the low strength of the exhuming body compared to the surrounding mantle, which nucleates the rift above it (for similar feedbacks inferred from analogue modelling, see Corti et al., 2003).

Importantly, the ascent of the UHP body is substantially triggered by the accompanying crustal extension and thinning, as we have confirmed by running an equivalent model with a 10× lower extension rate: for this slow extension rate the UHP body rises at only 1.7 mm/yr and eventually stalls and underplates the lithosphere, impeded by the relatively high viscosity of surrounding mantle (Rey et al., 2009; Weinberg and Podladchikov, 1994) (Fig. 4). This helps explain how a low-density body can remain lodged at depth, until a triggering event (such as extension) sufficiently weakens the overlying lithosphere by decreasing the effective viscosity, allowing it to ascend. The rise of the partially molten UHP body in Fig. 3 is intimately tied to rifting in a kind of positive feedback: 1) the positive buoyancy and low strength of the body at depth causes rifting to localise above it, and 2) the localisation reduces the effective viscosity of the rifted lithosphere. The reduction in strength of the rifting lithosphere results from strain-rate weakening (during non-linear dislocation creep) in the ductile lower crust and mantle, and frictional strain softening as shear zones form in brittle crust.

After the UHP body rises further to reach the lower crust (Fig. 3c) the rapid decrease in its average density and the density contrast to surrounding material starts to level off (Supplementary Note S1) and a proportion of the diapir spreads out laterally along the low-viscosity layer at the base of the crust (e.g., Hacker et al., 2011; Walsh and Hacker, 2004). At the same time, secondary normal faults form in the rift crust above it, near the margins of what will become the UHP-bearing gneiss dome. Despite some ponding at the Moho, most of the body still has sufficient buoyancy to rise into the upper crust. This rise causes a topographic dome (Fig. 3d) and a reversal in the dip of faults formed above it, like the inward-directed plastic slip lines seen in analogue models when indenting a layer of finite thickness (Merle and Donnadieu, 2000) (Fig. 3f(i)). Deformation is now localised above the body, yet the crust has not yet thinned by more than 20%, because it has largely been buoyed up, and it has in part been replaced by partial melt. At this point, the fraction of partial melt in the rising body reaches a maximum of ~40% (Fig. 3f(ii)), comparable to the observed volumes of in situ leucosomes and felsic dikes in the D'Entrecasteaux gneiss domes (Little et al., 2011).

The highest percentage of partial melt in the models occurs at shallow depths where pressures are lowest (Fig. 3f(ii)). Average densities in the zone of partial melt reduce to below 2600 kg m^{-3}, where exhumation rates reach 3–4 cm/yr, and briefly spike to higher values (Supplementary Note S1, Supplementary Fig. S2). After 2.3 Myr, the shallowest, HP part of the body has breached the surface whereas deeper-seated UHP rocks take 1 Myr longer to reach the brittle upper crust. Exhumation rates decline rapidly after this time, along with a more gradual decline in the average melt content of the body (Supplementary Note S1).

The P–T–t paths predicted by the modelling (Fig. 5) are broadly consistent with those from thermobarometry and geochronology (Baldwin et al., 2004, 2008). Further experiments indicate that the timing and degree to which buoyant ascent and outward-dipping indentation shear zones above the diapir dominate over more typical extension (as represented by inward-dipping rift-flanking shear zones, e.g., Fig. 3b) depend on the initial thermal structure, the rheology of the body and surrounding lithosphere, and the initial size of the body. For example, a larger diapiric body rises more rapidly, results in greater uplift of the surface, and causes more deformation of the medium surrounding the diapir (Fig. 6; Supplementary Fig. S3). As constrained by the observed time frame for (U)HP exhumation (4–8 Myr.), our model places upper and lower bounds on the size of the UHP body at depth. For our cross-sectional models with their assumed rheologies, we can constrain the radius of the body to be around 22 km, or an area of ca. 1500 km^2. However, the exhumation rate and partitioning of extensional deformation between the diapir

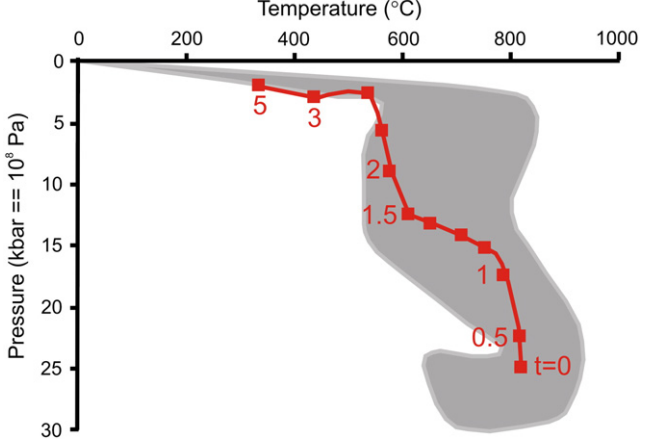

Fig. 5. Pressure–Temperature–time path for a tracer particle initially at x = 135 km, y = −90 km in the middle of the continental-affinity body (red line). Red numbers are time since exhumation started, in My. Pressure is computed as mean stress including dynamic stresses. For reference, smoothed PTt bounds for the retrograde path of exhumed rocks from Baldwin et al. (2004) are also shown (grey shading), where the estimated exhumation time (2.4 GPa to surface) was 4.3 My.

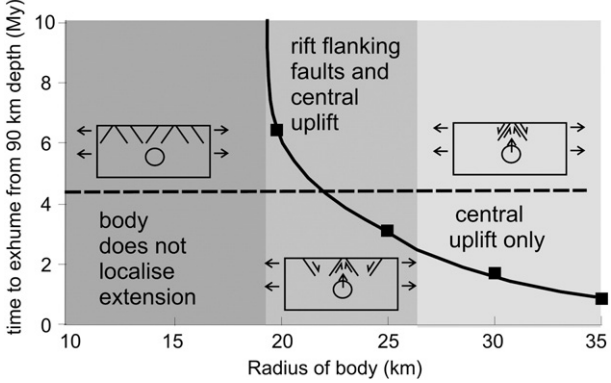

Fig. 6. Effect of subducted body dimensions on exhumation time and deformation style. Time for body to reach surface from 90 km depth, vs. initial size of circular body. Bodies below an initial radius of ca. 19 km do not localise extension and are not exhumed. Bodies with a radius of >26 km do not form initial rift-flanking faults, i.e. central uplift only (see schematised insets). Dashed horizontal line represents estimate of exhumation time from 2.4 GPa to surface from Baldwin et al. (2004).

and rift-flanking faults depend to some degree on the amount of strain softening prescribed in frictional crust and mantle (e.g., Buck and Lavier, 2001). A 2D model with less crustal strain-softening than in Fig. 3 experiences less extension along rift-flanking faults and more deformation surrounding the diapir, although the time for the diapir to reach the surface is not significantly affected. In models that have frictional mantle strain softening to the same degree as the crust, the diapir rises faster through the upper mantle, averaging a 50% greater exhumation rate.

The modelled pattern of brittle shear zones (faults) in the crust is dominated by rotated, low-angle, inward-dipping, rift-flanking faults, separated by the diapir that has buoyantly indented and punched through the brittle upper crust, resulting in outward-dipping, steep normal faults where the diapir breaches the surface (Fig. 3f(i)). This gross rift structure agrees broadly with that of the Woodlark rift, although the upper crust ("upper plate") of the latter is now mostly buried by volcanic rocks and sediments. The outer rift-flanking fault to the left of the exhumed UHP body in the model is compatible with the present location of the Goodenough Fault south of the D'Entrecasteaux Islands (Fig. 1; Supplementary Fig. S1). The rift symmetry in our model is related to the initial circular shape of the subducted body. An initially elongate, north-dipping UHP body favours more asymmetric rift development with the main rift boundary fault to the south, similar to the relationship observed between the UHP terranes and the Goodenough Fault in the Woodlark Basin (Supplementary Fig. S4). An initially north-dipping UHP body at depth is expected if emplacement of the UHP body resulted from northward subduction of the Australian continental margin. Rift asymmetry can also be enhanced by an initially thicker crust to the south, or by 3D rift propagation to the west (see discussion below).

Others have suggested that the presence of a dense, ultramafic layer up to 20 km thick (the Papuan Ultramafic Belt (PUB), which was obducted onto the Australian margin at the end of the subduction phase at 50 Ma) created a density inversion that aids the rise of buoyant partial melt through the upper lithosphere (Martinez et al., 2001). To test this idea, we ran additional 2D models (not shown) that incorporated a dense, high-strength PUB layer (our ophiolite density taken as 3000 kg m^{-3} similar to that used by Martinez et al., 2001; and with a viscosity 10 times that of the surrounding continental crust). Surprisingly, we did not find that a denser uppermost plate made a significant difference to the rate or manner of diapiric ascent, perhaps because the PUB is mostly situated in the upper crust, where it is cold and brittle (Davies, 1980a; Davies and Jacques, 1984) and therefore is unlikely to cause viscous overturning via a density inversion. That is, as long as the diapir is below the high-density lid, the net effect on pressure gradients around the body is small. By the time it reaches the dense layer, deformation is mostly brittle and does not obey the simple prediction for viscous overturning via density inversion, but is instead exhumed by brittle faulting.

Tomographic studies of the Woodlark Rift (Abers et al., 2002; Ferris et al., 2006) show that the continental crust beneath the D'Entrecasteaux Islands has thinned to ca. 20 km, compared to >30 km thickness along the margins of the rift to the north and south. Abers et al. (2002) suggested that the 10–15 km of crustal thinning beneath the islands has been compensated isostatically at depth by insertion of anomalously low-density upper mantle, allowing this part of the continental rift to remain emergent. By contrast, in our simplified

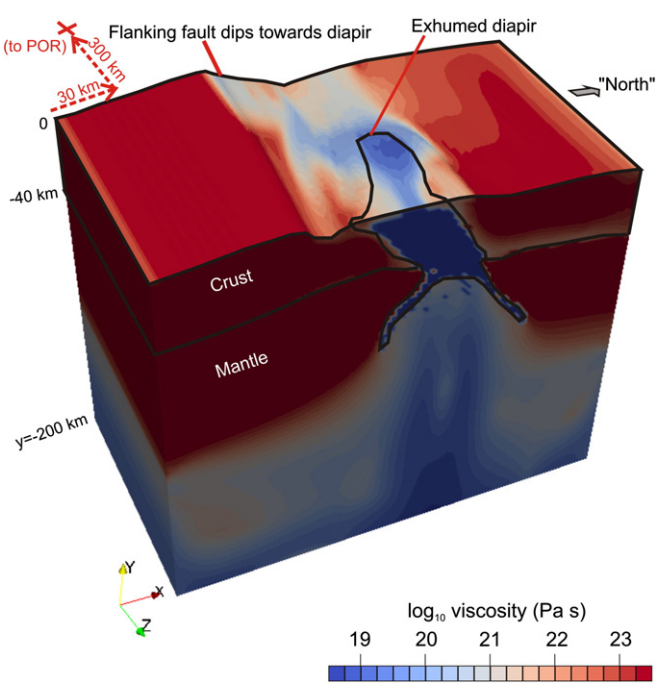

Fig. 7. Colour contours of log10 (effective viscosity) for 3D model after 1.9 My extension. The model setup is shown in Fig. 2b. Eclogite-facies diapiric body outlined in bold black line. No vertical exaggeration.

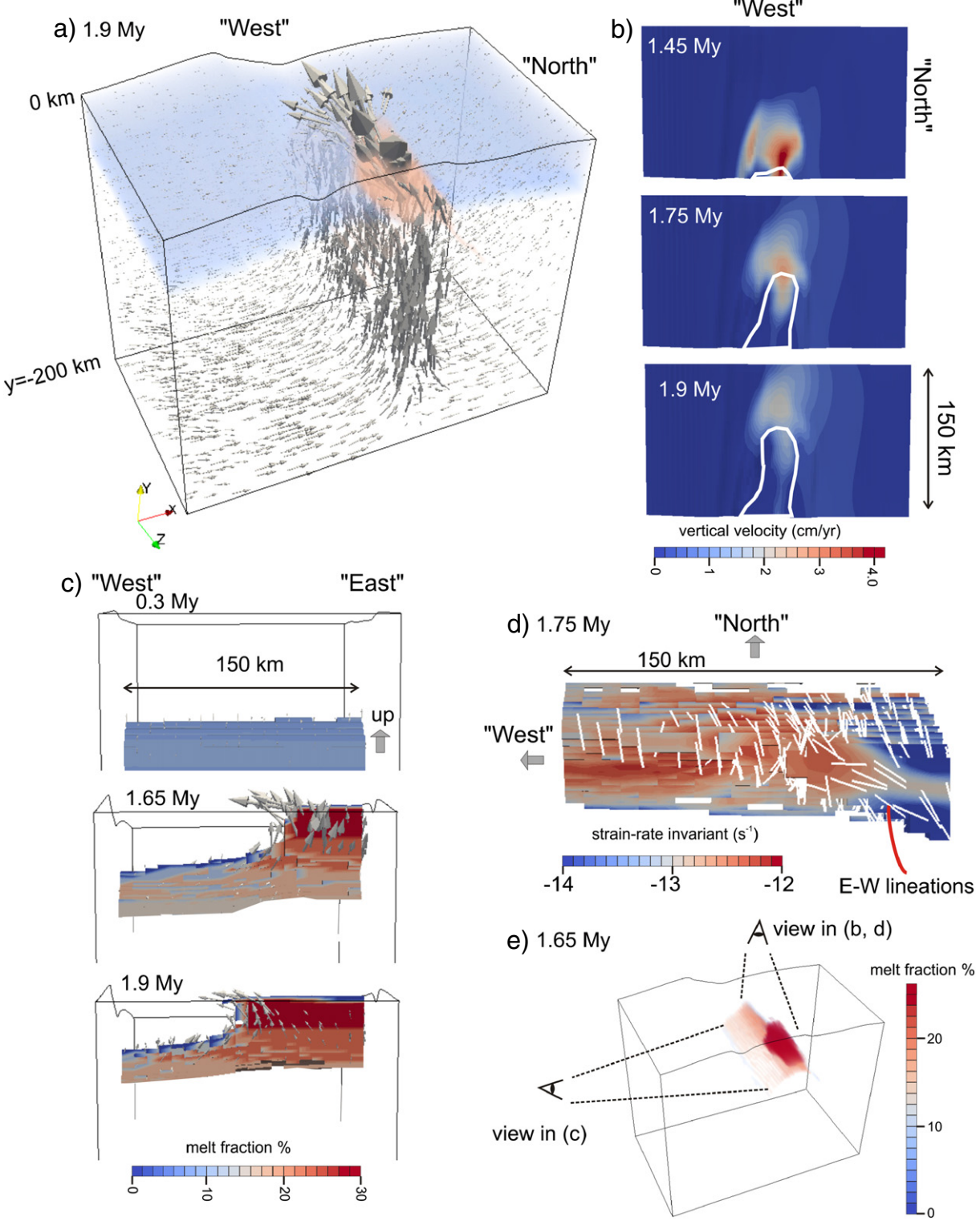

Fig. 8. Results of the 3D numerical model with the setup from Fig. 2(b). (a) Materials and flow vectors after 1.9 My extension for the 3D model. Mantle material is not coloured. Brown = diapiric body, blue = upper and lower crust. Maximum vector magnitude is 18 cm yr^{-1}. (b) Vertical uplift rate contours at 1.45, 1.75 and 1.9 My looking down onto the top surface of the model, showing progressive westward migration of buoyant exhumation and vertical uplift (red contours). Bold white line outlines exhumed body. (c) Progressive evolution in location and melt percentage of diapiric body from east to west, shown looking at a slice through the middle of the body from the south (viewpoint shown in (e)). A subset of flow vectors are shown in grey (maximum magnitude is 43 cm/yr) and indicate upward flow at depth giving way to along-axis flow as body progressively enters the crust from east to west. Flat section at top of body after 1.65, 1.9 My represents intersection of the body with the surface. (d) Planform view showing a subset of principal creep stretch directions (white bars) projected onto a horizontal plane at the top of the diapiric body after 1.75 My; viewpoint shown in (e). Along-axis (east–west, E–W) oriented stretching lineations occur at the top of the body in the east where it has risen to the surface; these formed at shallow depths just prior to embrittlement, owing to along-strike flow and vertical squeezing.(e) Melt fraction and perspective view of diapiric body, at 1.65 My.

2D model, buoyant felsic material and partial melt from eclogitic-facies rocks replaces and supports the thinned continental crust of the rift (Fig. 3f(ii)). The effect of reduced mantle density is present in our model, but is secondary and is not required to explain the topography of the domes.

4.2. 3D model results

Conceivably, some or all of the spatial trends seen near the D'Entrecasteaux Islands – namely, the westward progression in ages of extension and exhumation – may have been controlled by the westward propagation of the Woodlark seafloor-spreading system, and/or by that system's nearby pole of rotation, such that the rate of extension increases eastward away from the nearby pole of rotation (Fig. 1). To investigate the influence of an along-strike gradient in extension rate on along-strike variation in UHP exhumation, we ran a lower resolution 3D model (Fig. 2b).

The 3D model imposes boundary velocities consistent with the 3.5–0.5 Ma relative pole of rotation between the Australian and Woodlark plates ca. 500 km west of the actively spreading rift (Benes et al., 1994; Taylor et al., 1999) (Fig. 1). The UHP body is initially emplaced as a cylinder with a radius of 22 km, at a depth of 90 km. As in the 2D models, extensional faulting develops as rifting localises over the top of the buoyant body (Fig. 7). However, in the 3D model the initial rift faulting occurs preferentially on the south side of the exhuming diapir. This asymmetry results from the location of the pole of rotation, which is south and west of the axis of the rising crustal body. As well as the asymmetry, the location of the pole of rotation causes greater extensional plate rates in the east. Because the ascent of the buoyant body is aided by extension, and extensional plate motion increases eastward, the 3D model causes the initially uniform diapir to rise faster in the east (Figs. 7 and 8).

The extensional strain-rate variation from east to west is the key to many of the along-strike changes in the model; in particular, it causes the locus of diapiric exhumation and topographic uplift to begin in the east. After this first-exhumed body of partially molten material cools, it freezes into a brittle deforming plug. Meanwhile the still-molten material farther west, which has taken longer to reach the surface, is still experiencing buoyant uplift and rises vertically, shifting the locus of uplift and exhumation westward (Fig. 8b–c). Moreover, the more advanced decompression melting in the east causes stronger buoyancy forces there, reinforcing eastward ductile flow of the UHP body relative to the overlying crustal lid. As a result of this lateral ductile flow, the direction of maximum finite extension (creep strain) is east–west in the upper part of the body, and roughly parallel to the rift margins and perpendicular to the extension direction. Intriguingly, this provides an explanation for one of the most conspicuous and counter-intuitive structural features of the domes: the strongly longitudinal (rift-margin parallel) trend of stretching lineations in the exhumed gneisses (Little et al., 2011). The models also predict a swing to a progressively more N–S trend of finite stretching around the edges of the domes (Fig. 8d) as is also observed in the field (Little et al., 2011), (e.g., lineation trends on Goodenough and Mailolo domes as plotted in Supplementary Fig. S1). Without an imposed (plate motion related) velocity gradient along strike, and with a much higher model resolution, it is possible that the original cylindrical body at depth would fragment into a coeval array of quasi-periodic Raleigh–Taylor instabilities.

5. Discussion and conclusions

This study has highlighted the positive feedback that can occur between extension and the diapiric rise of partially molten crust through the lithosphere. We have shown how a weak, low-viscosity body at depth can cause rifting to localise above it, promoting extension that further weakens the overlying lithosphere, allowing the positively buoyant partially molten body to rise rapidly from depth. Our numerical models, while simplifying the conditions experienced by rocks in the Woodlark Basin, show that the geologically observed rates (2–3 cm/yr) and style of (U)HP exhumation are physically consistent with the diapiric rise of buoyant UHP bodies that contain partial melt. In particular, we are able to explain (1) the observed pressure–temperature evolution of HP and UHP rocks; (2) rapid exhumation rates of 2–3 cm/yr as a result of partial melt causing a reduction in density, and a complex feedback between viscosities, extension rates and melt fraction in the diapir; (3) flow patterns and structure of diapiric domes broadly consistent with that seen in the D'Entrecasteaux Islands; (4) buoyant support and high elevation of thinned crust due to the presence of an underlying partially molten UHP body and elevated temperatures in crust and mantle, consistent with observations from tomography; (5) asymmetry in initial flanking rift structure (for an initially dipping subducted body, and as a result of 3D rotations, e.g., Fig. 7 and Supplementary Fig. S4); and (6) westward propagation of rifting and exhumation. The 3D model also illustrates how viscous flow associated with variable along-strike extension rates is consistent with observed ductile fabrics indicating rift margin-parallel stretching of those rocks when they were in the lower crust.

Alternative explanations for exhumation of UHP rocks in the Woodlark Basin are not as well supported by geological evidence. Eduction (Andersen et al., 1991), whereby the subduction suture is reactivated as a major normal fault along which the domes have been exhumed asymmetrically (e.g., Webb et al., 2008) is not supported by structural mapping, which documents ductile flow orthogonal to the plate motion direction together with dominantly irrotational (bulk pure shear) vertical ductile thinning in the upper part of the domes (Little et al., 2011). Exhumation along a subduction channel during ongoing contraction (e.g., Gerya and Stockhert, 2006; Warren et al., 2008) is ruled out because exhumation of the domes occurred after collision had ceased, in the late Neogene during a time of regional extension in the Woodlark rift when there is little or no evidence for ongoing subduction, either along the ancient Australian–Woodlark plate boundary near the Papuan Peninsula or the Trobriand trough to the north (Abers and Roecker, 1991; Hall and Spakman, 2002; Kirchoff-Stein, 1992). The gneiss domes appear to have ascended vertically as diapirs through overlying layers, while stalling and flowing laterally along the rift after reaching lower crustal depths, rather than being exhumed in a slab-like, asymmetric manner as a result of unidirectional slip or shearing in a subduction channel (cf. Baldwin et al., 2004).

The Woodlark Basin hosts the only example of recently exhumed (U)HP rocks, and yet the most commonly advocated mechanism for UHP exhumation – extrusion or buoyant rise of coherent nappes within a subduction channel during ongoing plate convergence – does not appear to be operating in this uniquely young and well-understood setting. Although extension has been implicated in the exhumation of lower crust in metamorphic core complexes and gneiss domes (e.g., Fayon et al., 2004; Rey et al., 2009; Tirel et al., 2004) and the rise of salt diapirs (e.g., Vendeville and Jackson, 1992), it has not been suggested as a necessary ingredient for the diapiric rise of (U)HP rocks from mantle depths. Could it be that other, more ancient and less well understood UHP terranes were similarly exhumed after plate convergence had ceased, and during subsequent phases of a Wilson cycle? (e.g., Hacker, 2007; Johnston et al., 2007; Walsh and Hacker, 2004; Yin et al., 2007).

If so, there is a need to explain how UHP and HP mineral assemblages, created during the subduction phase, could be preserved until their ascent through the crust. Perhaps thermal refrigeration from the previous subduction phase prevents retrogression until mechanical and thermal effects of a propagating rift sufficiently soften the overlying lithosphere to allow the ascent of a deeply buried buoyant crustal body that partially melts during ascent (e.g., Little et al.,

2011). More complex models incorporating a transition from subduction to extension are required to investigate this process (cf. Burov et al., 2001; Li and Gerya, 2009). Nevertheless, we have shown to first order that the Woodlark Basin (U)HP exhumation can be simply explained in terms of diapiric flow aided by and interacting with a propagating extensional rift.

Supplementary materials related to this article can be found online at doi:10.1016/j.epsl.2011.09.031.

Acknowledgments

This study was funded by Marsden Fund grant 08-VUW-020 to T.A.L., L.W., and S.E., and NSF grant EAR-0607775 to B.H. Field and logistical assistance were provided by Neville Palmer, Megan Korchinski, Stacia Gordon, members of the National Mapping Bureau of Papua New Guinea, Willie Solomon, and the crew and captain of the *MV Jazz II*. Cooperation of the villagers, local area managers, councillors and school staff throughout the D'Entrecasteaux Islands and Papuan Peninsula is gratefully acknowledged. We acknowledge useful discussions with Hugh Davies, Stacia Gordon, Geoff Abers, Ian Smith, Suzanne Baldwin, and Paul Mann. Constructive reviews were received from Roberto Weinberg and Roger Buck.

References

Abers, G.A., Roecker, S.W., 1991. Deep structure of an arc–continent collision: earthquake relocation and inversion for upper mantle P and S wave velocities beneath Papua New Guinea. J. Geophys. Res. 96, 6379–6401.

Abers, G.A., Ferris, A., Craig, M., Davies, H., Lerner-Lam, A., Mutter, J.C., Taylor, B., 2002. Mantle compensation of active metamorphic core complexes at Woodlark rift in Papua New Guinea. Nature 418, 862–865.

Amato, J.M., Johnson, C.M., Baumgartner, L.P., Beard, B.L., 1999. Rapid exhumation of the Zermatt Saas ophiolite deduced from high precision Sm/Nd and Rb/Sr geochronology. Earth Planet. Sci. Lett. 171, 425–438.

Andersen, T.B., Jamtveit, B., 1990. Uplift of deep crust during orogenic extensional collapse: a model based on field studies in the Sogn-Sunnifjord region of western Norway. Tectonics 9, 1097–1111.

Andersen, T.B., Jamtveit, B., Dewey, J.F., Swensson, E., 1991. Subduction and eduction of continental crust; major mechanisms during continent–continent collision and orogenic extensional collapse. Terra Nova 3, 303–310.

Baldwin, S.L., Ireland, T.R., 1995. A tale of two eras: Plio-Pleistocene unroofing of Cenozoic and late Archean zircons from active metamorphic core complexes, Solomon Sea, Papua New Guinea. Geology 23, 1023–1026.

Baldwin, S.L., Monteleone, B., Webb, L.E., Fitzgerald, P.G., Grove, M., Hill, J., 2004. Pliocene eclogite exhumation at plate tectonic rates in eastern Papua New Guinea. Nature doi:10.1038, 8 pp.

Baldwin, S.L., Rawling, T., Fitzgerald, P.G., 2007. Thermochronology of the New Caledonian HP terrane: implications for mid-Tertiary plate boundary processes in the SW Pacific. GSA Spec. Pap. 419, 117–134.

Baldwin, S.L., Webb, L.E., Monteleone, B.D., 2008. Late Miocene coesite–eclogite exhumed in the Woodlark Rift. Geology 36, 735–738.

Benes, V., Scott, S.D., Binns, R.A., 1994. Tectonics of rift propagation into a continental margin: Western Woodlark Basin, Papua New Guinea. J. Geophys. Res. 99, 4439–4455.

Brace, W.F., Kohlstedt, D.L., 1980. Limit on lithospheric stress imposed by laboratory experiments. J. Geophys. Res. 85, 6248–6252.

Buck, W.R., Lavier, L.L., 2001. A tale of two kinds of normal fault: the importance of strain weakening in fault development. Geol. Soc. Lond. Spec. Publ. 187, 289–303. doi:10.1144/GSL.SP.2001.187.01.14.

Buiter, S.J.H., Pfiffner, O.A., Beaumont, C., 2009. Inversion of extensional sedimentary basins: a numerical evaluation of the localisation of shortening. Earth Planet. Sci. Lett. 288, 492–504. doi:10.1016/j.epsl.2009.10.011.

Burov, E., Jolivet, L., Le Pourhiet, L., Poliakov, A., 2001. A thermomechanical model of exhumation of high pressure (HP) and ultra-high pressure (UHP) metamorphic rocks in Alpine-type collision belts. Tectonophysics 342, 113–136.

Chopin, C., 1984. Coesite and pure pyrope in high-grade blueschists of the Western Alps: a first record and some consequences. Contrib. Mineralog. Petrol. 86, 107–118.

Chopin, C., 2003. Ultrahigh-pressure metamorphism: tracing continental crust into the mantle. Earth Planet. Sci. Lett. 212, 1–14.

Connolly, J.A.D., Petrini, K., 2002. An automated strategy for calculation of phase diagram sections and retrieval of rock properties as a function of physical conditions. J. Metamorph. Petrol. 20, 697–708.

Corti, G., Bonini, M., Conticelli, S., Innocenti, F., Manetti, P., Sokoutis, D., 2003. Analogue modelling of continental extension: a review focused on the relations between the patterns of deformation and the presence of magma. Earth Sci. Rev. 63, 169–247.

Daczko, N.R., Caffi, P., Halpin, J.A., Mann, P., 2009. Metamorphic evolution of the Dayman Dome metamorphic core complex, eastern Papua New Guinea. J. Metamorph. Geol. 27, 405–422.

Davies, H.L., 1980a. Folded thrust fault and associated metamorphics in the Suckling–Dayman massif, Papua New Guinea. Am. J. Sci. 280A, 171–191.

Davies, H.L., 1980b. Crustal structure and emplacement of ophiolite in southeastern Papua New Guinea. Colloques Internationaux du C.N.R.S. 272, 17–33.

Davies, H.L., 1990. Structure and evolution of the border region of New Guinea. In: Carman, G.J., Carman, Z. (Eds.), Petroleum Exploration in Papua New Guinea: Proceedings of the First PNG Petroleum Convention, Port Moresby, February 12–14, 1990, pp. 249–269.

Davies, H.L., Jacques, A.L., 1984. Emplacement of ophiolite in Papua New Guinea. Geol. Soc. Lond. Spec. Publ. 13, 341–350.

Davies, H., Warren, R.G., 1988. Origin of eclogite-bearing, domed, layered metamorphic complexes ("core complexes") in the D'Entrecasteaux islands, Papua New Guinea. Tectonics 7, 1–21.

Dobrzhinetskaya, L.F., Eide, E.A., Larsen, R.B., Sturt, B.A., Trønnes, R.G., Smith, D.C., Taylor, W.R., Posukhova, T.V., 1995. Microdiamond in high-grade metamorphic rocks of the Western Gneiss region, Norway. Geology 23, 597–600.

Dziewonski, A.M., Anderson, D.L., 1981. Preliminary earth reference model. Phys. Earth Planet. Inter. 25, 297–356.

Fayon, A.K., Whitney, D.L., Teyssier, C., 2004. Exhumation of orogenic crust: diapiric ascent versus low-angle normal faulting. GSA Spec. Pap. 380, 129–140.

Ferris, A., Abers, G.A., Zelt, B., Taylor, B., Roecker, S., 2006. Crustal structure across the transition from rifting to spreading: the Woodlark rift system of Papua New Guinea. Geophys. J. Int. 166, 622–634.

Fitzgerald, P.G., Baldwin, S.L., Miller, S.L., Perry, S.E., Webb, L.E., Little, T.A., 2008. Low-Temperature Constraints on the Evolution of Metamorphic Core Complexes of the Woodlark Rift System, Annual Meeting of the American Geophysical Union. AGU, EOS Transactions, San Francisco, CA.

Fullsack, P., 1995. An arbitrary Lagrangian–Eulerian formulation for creeping flows and applications in tectonic models. Geophys. J. Int. 120, 1–23.

Gerya, T.V., Stockhert, B., 2006. Two-dimensional numerical modeling of tectonic and metamorphic histories at active continental margins. Int. J. Earth Sci. 95, 250–274.

Gerya, T.V., Yuen, D.A., 2003. Characteristics-based marker-in-cell method with conservative finite-differences schemes for modeling geological flows with strongly variable transport properties. Phys. Earth Planet. Inter. 140, 293–318.

Goetze, C., 1978. The mechanisms of creep in olivine. Philos. Trans. R. Soc. Lond. B288, 99–119.

Goodliffe, A., Taylor, B., Martinez, F., Hey, R., Maeda, K., Ohno, K., 1997. Synchronous reorientation of the Woodlark basin spreading center. Earth Planet. Sci. Lett. 146, 233–242.

Hacker, B.R., 2007. Ascent of the ultrahigh-pressure Western Gneiss Region, Norway. GSA Spec. Pap. 419, 171–184.

Hacker, B.R., Peacock, S.M., 1994. Creation, preservation, and exhumation of ultrahigh pressure metamorphic rocks. In: Coleman, R.G., Wang, X. (Eds.), Ultrahigh Pressure Metamorphism. Cambridge University Press, pp. 159–181.

Hacker, B.R., Ratschbacher, L., Webb, L., Shuwen, D., 1995. What brought them up? Exhumation of the Dabie Shan ultrahigh-pressure rocks. Geology 23, 743–746.

Hacker, B.R., Kelemen, P.B., Behn, M.D., 2011. Differentiation of the continental crust by relamination. Earth Planet. Sci. Lett. doi:10.1016/j.epsl.2011.05.024.

Hall, R., Spakman, W., 2002. Subducted slabs beneath Eastern Indonesia–Tonga region: insights from tomography. Earth Planet. Sci. Lett. 201, 321–336.

Hermann, J., Rubatto, D., Korsakov, A., Shatsky, V.S., 2001. Multiple zircon growth during fast exhumation of diamondiferous, deeply subducted continental crust (Kokchetav Massif, Kazakhstan). Contrib. Mineralog. Petrol. 141, 66–82.

Hill, E.J., 1994. Geometry and kinematics of shear zones formed during continental extension in eastern Papua New Guinea. J. Struct. Geol. 16, 1093–1105.

Hill, E.J., Baldwin, S.L., Lister, G.S., 1995. Magmatism as an essential driving force for formation of active metamorphic core complexes in eastern Papua New Guinea. J. Geophys. Res. 100, 10441–10452.

Johnston, S.M., Hacker, B.R., Anderson, T.B., 2007. Exhuming ultrahigh-pressure rocks: overprinting extensional structures and the role of the Nordfjord–Sogn Detachment Zone. Tectonics 26, TC5001.

Kaus, B.J.P., Mühlhaus, H., May, D.A., 2010. A stabilization algorithm for geodynamic numerical simulations with a free surface. Phys. Earth Planet. Inter. 181, 12–20.

Kirchoff-Stein, K.S., 1992. Seismic reflection study of the New Britain and Trobriand subduction systems and their zone of initial contact in the western Solomon Sea. (PhD dissertation). University of California, Santa Cruz, Santa Cruz, California.

Li, Z., Gerya, T.V., 2009. Polyphase formation and exhumation of high- to ultrahigh-pressure rocks in continental subduction zone: numerical modeling and application to the Sulu ultrahigh-pressure terrane in eastern China. J. Geophys. Res. 114, B09406. doi:10.1029/2008JB005935.

Liou, J.G., Tsujimori, T., Zhang, R.Y., Katayama, I., Maruyama, S., 2004. Global UHP metamorphism and continent subduction/collision: the Himalayan model. Int. Geol. Rev. 46, 1–27.

Little, T.A., Baldwin, S.L., Fitzgerald, P.G., Monteleone, B., 2007. Continental rifting and metamorphic core complex formation ahead of the Woodlark Spreading Ridge, D'Entrecasteaux Islands, Papua New Guinea. Tectonics 26, TC1002. doi:10.1029/2005TC001911.

Little, T.A., Hacker, B.R., Gordon, S.M., Baldwin, S.L., Fitzgerald, P.G., Ellis, S., Korchinski, M., 2011. Diapiric exhumation of Earth's youngest (UHP) eclogites in the gneiss domes of the D'Entrecasteaux Islands, Papua New Guinea. Tectonophysics 510, 39–68.

Lus, W.Y., McDougall, I., Davies, H.L., 2004. Age of the metamorphic sole of the Papuan Ultramafic Belt ophiolite, Papua New Guinea. Tectonophysics 392, 85–101.

Martinez, F., Goodliffe, A., Taylor, B., 2001. Metamorphic core complex formation by density inversion and lower crustal extrusion. Nature 411, 930–933.
Merle, O., Donnadieu, F., 2000. Indentation of volcanic edifices by the ascending magma. Geol. Soc. Lond. Spec. Publ. 174, 43–53.
Monteleone, B.D., Baldwin, S.L., Webb, L.E., Fitzgerald, P.G., Grove, M., Schmitt, A.K., 2007. Late Miocene–Pliocene eclogite-facies metamorphism, D'Entrecasteaux Islands, SE Papua New Guinea. J. Metamorph. Geol. 25, 245–265.
Mutter, J.C., Mutter, C.Z., Fang, J., 1996. Analogies to oceanic behaviour in the continental breakup of the western Woodlark Basin. Nature 380, 333–336.
Parrish, R.R., Gough, S.J., Searle, M.P., Waters, D.J., 2006. Plate velocity exhumation of ultrahigh-pressure eclogites in the Pakistan Himalaya. Geology 34, 989–992.
Pelletier, D., Fortin, A., Camarero, R., 1989. Are FEM solutions of incompressible flows really incompressible? (or how simple flows can cause headaches!). Int. J. Numer. Meth. Fluids 9, 99–112.
Quinquis, M.E.T., Buiter, S.J.H., Ellis, S., 2011. The role of boundary conditions in numerical models of subduction zone dynamics. Tectonophysics 497, 57–70. doi:10.1016/j.tecto.2010.11.001.
Rey, P.F., Teyssier, C., Whitney, D.L., 2009. Extension rates, crustal melting, and core complex dynamics. Geology 37, 391–394.
Rogerson, R., Hilyard, D., Finalyson, E.J., Holland, D.S., Nion, S.T.S., Sumaiang, R.S., Duguman, J., Loxton, C.D.C., 1987. The geology and mineral resources of the Sepik headwaters region, Papua New Guinea. Papua New Guinea Geological Surveys Memoir, 12.
Rosenberg, C.L., Medvedev, S., Handy, M.R., 2007. Effects of melting on faulting and continental deformation. In: Handy, M.R., Hirth, G., Hovius, N. (Eds.), Tectonic Faults: Agents of Change on a Dynamic Earth, Report of the 95th Dahlem workshop on The Dynamics of Fault Zones, Berlin, January 16–21, 2005, pp. 357–402.
Smith, D.C., 1984. Coesite in clinopyroxene in the Caledonides and its implications for geodynamics. Nature 310, 641–644.
Spencer, J.E., 2010. Structural analysis of three extensional detachment faults with data from the 2000 Space-Shuttle Radar Topography Mission. GSA Today 20, 1–10.
Taylor, B., Huchon, P., 2002. Active continental extension in the western Woodlark basin: a synthesis of Leg 180 results. In: Huchon, P., Taylor, B., Klaus, A. (Eds.), Proceedings of the Ocean Drilling Program, Scientific Results, Volume 180. Ocean Drilling Program, Texas A & M University, College Station, Texas, pp. 1–36 (CD ROM).
Taylor, B., Goodliffe, A.M., Martinez, F., 1999. How continents break-up: insights from Papua New Guinea. J. Geophys. Res. 104, 7497–7512.
Tirel, C., Brun, J.-P., Burov, E., 2004. Thermomechanical modeling of extensional gneiss domes. GSA Spec. Pap. 380, 67–78.
Tregoning, P., Lambeck, K., Stolz, A., Morgan, P., McClusky, S.C., van der Beek, P., McQueen, H., Jackson, R.J., Little, R.P., Laing, A., Murphy, B., 1998. Estimation of current plate motions in Papua New Guinea from global positioning system observations. J. Geophys. Res. 103, 12181–12203.
Van Ufford, Q.A., Cloos, M., 2005. Cenozoic tectonics of New Guinea. AAPG Bull. 89, 119–140.
Vendeville, B.C., Jackson, M.P.A., 1992. The rise of diapirs during thin-skinned extension. Mar. Petrol. Geol. 9, 331–353.
Vrijmoed, J.C., Podladchikov, Y.Y., Andersen, T.B., Hartz, E.B., 2009. An alternative model for ultra-high pressure in the Svartberget Fe–Ti garnet–peridotite, Western Gneiss Region, Norway. Eur. J. Mineral. 21, 1119–1133.
Wallace, L.M.L.M., Stevens, C., Silver, E., McCaffrey, R., Loratung, W., Hasiata, S., Stanaway, R., Curley, R., Rosa, R., Taugaloidi, J., 2004. GPS and seismological constraints on active tectonics and arc–continent collision in PNG: implications for mechanics of microplate rotations in a plate boundary zone. J. Geophys. Res. 109. doi:10.1029/2003JB002481.
Walsh, E.O., Hacker, B., 2004. The fate of subducted continental margins: two-stage exhumation of the HP to UHP Western Gneiss Complex, Norway. J. Metamorph. Geol. 22, 671–689.
Warren, C.J., Beaumont, C., Jamieson, R.A., 2008. Modelling tectonic styles and ultra-high pressure (UHP) rock exhumation during the transition from oceanic subduction to continental collision. Earth Planet. Sci. Lett. 267, 129–145.
Webb, L.E., Baldwin, S.L., Little, T.A., Fitzgerald, P.G., 2008. Can microplate rotation drive subduction inversion? Geology 36, 823–826.
Weinberg, R.F., Podladchikov, Yu., 1994. Diapiric ascent of magmas through power–law crust and mantle. J. Geophys. Res. 99, 9543–9559.
Yin, A., Manning, C.E., Lovera, O., Menold, C.A., Xuanhua, C., Gehrels, G.E., 2007. Early Paleozoic tectonic and thermomechanical evolution of ultrahigh-pressure (UHP) metamorphic rocks in the northern Tibetan Plateau, Northwest China. Int. Geol. Rev. 49, 681–716.
Zirakparvar, N.A., Baldwin, S., Vervoor, J.D., Fitzgerald, P.G., 2009. Lu–Hf dating of garnet from MCC's in the Woodlark Rift of southeastern Papua New Guinea. Abstract V43D-2291 presented at 2009 Fall Meeting, AGU, San Francisco, California, 14–18 Dec.
Zirakparvar, N.A., Baldwin, S., Fitzgerald, P.G., Vervoort, J.G., 2010. Piecing together the eastern Australia margin in Gondwana: origin of metamorphic rocks in the Woodlark Rift, SE Papua New Guinea. Abstract T13C-2220 presented at 2010 Fall Meeting, AGU, San Francisco, California, 13–17 Dec.